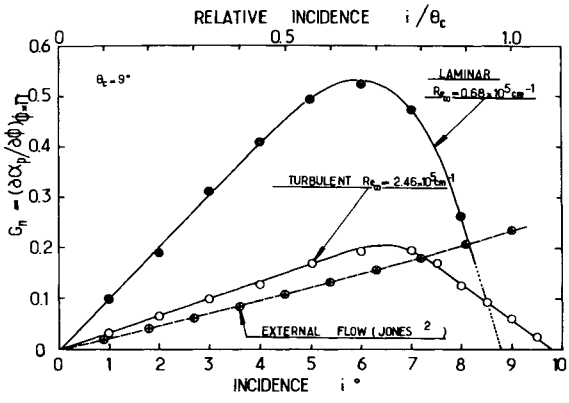

Fig. 4 Evolution of $(\partial\alpha_p/\partial\phi)_{\phi=\pi}$ with incidence angle.

parameter increases with incidence up to $i = 14°$ and becomes nearly constant beyond this value at about 0.33. The ratio of turbulent parameter G_o to the inviscid one is constant and close to 1.80 up to $i = 11°$ which is the limit value of Jones' data. The laminar values are about twice the turbulent ones and are slightly affected by Mach numbers as shown when comparing data previously obtained at $M_\infty = 6.85$, $Re_\infty = 0.25 \times 10^5$ cm^{-1} with those obtained under the present conditions.

The comparison of present results with data of Rainbird[5] for the turbulent case, shows a similar effect of Mach number. The maximum value of α_p follows the same evolution with incidence as the parameter G_o (Fig. 3). According to the results of Rainbird,[5] the Mach number effect appears to be different, whereas the present data point out a similar effect in the laminar case.

The α_p slope G at $\phi = \pi$ is particularly interesting for the determination of the separation incidence i_{sep}. Its evolution with incidence (Fig. 4), increasing linearly within $0 < i < 6°$ and decreasing linearly within $7° < i < i_{sep}$, presents a maximum value for $i = 6.5°$. Thus, the separation incidence is found equal to $9.8° = 1.09\ \theta_c$ with an accuracy estimate of $\pm 0.05°$. The laminar value obtained with less precision because of the minor frequency of measurements, is close to 8.8°, which means that the turbulent separation occurs 1° sooner than the laminar one. Furthermore, it is to be noted that the comparison between the experiments and the inviscid theory brings out a particular value of incidence angle (6°) beyond which the boundary effects are fundamental with respect to the separation phenomenon.

Finally, the separation azimuth ϕ_{sep}, deduced from the circumferential surface flow angle, decreases with incidence down to a constant value beyond $i = 14°$ (Fig. 5). This constant value seems to be slightly higher for the laminar case than for the turbulent case. In order to show the Mach number effect, some previous data have been plotted in the figure.

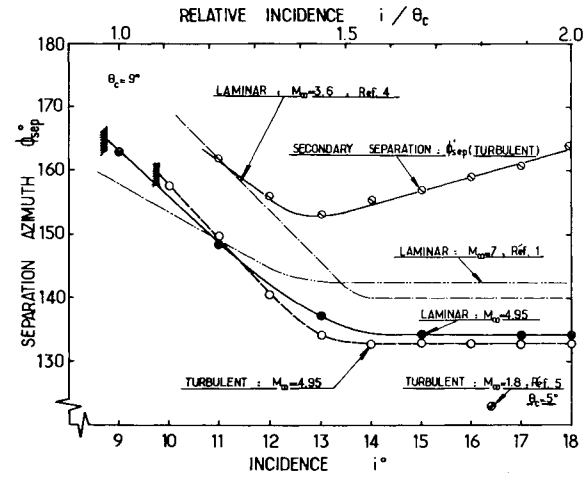

Fig. 5 Location of separation line. All data concern primary separation, except the symbol θ as indicated.

References

[1] Marcillat, J., "Etude Expérimentale du Sillage Proche d'un Cône Élancé en Incidence," Thèse de Doctorat es Sciences, July 1970, Université de Provence, Marseille, France; also see Publications Scientifiques et Techniques, n° 71-3, CEDOCAR Editions, Paris, France.

[2] Jones, D. J., "Numerical Solution of the Flow Field for Conical Bodies in a Supersonic Stream," Aèro. Rept. LR 507, July 1968, National Research Council of Canada, Ottawa, Ontario, Canada.

[3] Eichelbrenner, E. A. and Oudart, A., "Méthode de Calcul de la Couche Limite Tridimensionnelle," Publ. 76, 1955, Office National d'Etudes et de Recherches Aérospatiales, France.

[4] Avduevsky, V. S. and Medvedev, K. I., "Investigation of the Laminar Flow Separation on a Cone under Angle of Attack," Izvestia ANSSR, *Fluid and Gas Mechanics*, No. 3, 1966, pp. 117–119.

[5] Rainbird, W. J., "The External Flow Field about Yawed Circular Cones," AGARD Conference Proceedings No. 30, 1968, pp. 19-1–19-18.

[6] Feldhuhn, R. H. and Pasiuk, L., "An Experimental Investigation of the Aerodynamic Characteristics of Slender Hypersonic Vehicles at High Angles of Attack," NOLTR 68-52, May 1968, U.S. Naval Ordnance Lab., White Oak, Silver Springs, Md.

[7] Marcillat, J. and Roux, B., "Experimental and Theoretical Study of Supersonic Viscous Flow over a Yawed Cone," *AIAA Journal*, Vol. 10, No. 12, Dec. 1972, pp. 1625–1630.

Instantaneous Velocity Measurements in the Near Wake of a Helicopter Rotor

CHRISTIAN MARESCA,* DANIEL FAVIER,† AND JEAN REBONT‡
Institut de Mécanique des Fluides de Marseille, Marseille, France

A RECENT study on the near flow behind a propeller[1] has shown that the form of the mean velocities measured just downstream of the rotation plane can illustrate the significant phenomena which occur upon the blades. Such a method seemed to be applicable to a helicopter rotor wake. However, the unsteady nature of such a flow requires that the instantaneous velocities be measured.

The three instantaneous velocity components have been measured by use of a hot film wedge-shaped probe, located in the near wake of a two-bladed rotor tilted at $-10°$ as shown in Fig. 1. The untwisted blade (profile NACA 0018) has a rectangular shape. During all the tests the blade tip speed ωR (where ω is the angular frequency and R the radius of the rotor) and the wind-tunnel velocity were maintained respectively at 105 m/sec and 25 m/sec, so that the advance ratio was kept at a constant value (0.24). The sensor element of the probe was placed in the retreating blade zone at the position $0.25R$ from the rotation axis and $0.1R$ under the horizontal plane (see Fig. 1). The measurement method of the three velocity components by use of such a probe is described in Ref. 2. This method is applicable when the angle between the axis of the probe and the mean velocity direction is less than 12°. In our experiments,

Received February 26, 1974. This work was supported by "Direction des Recherches et Moyens d'Essais" under Contract D.R.M.E. 72/348.
Index category: Rotary Wing Aerodynamics.

* Chargé de Recherche au CNRS.

† Docteur de Spécialité.

‡ Ingénieur au CNRS.

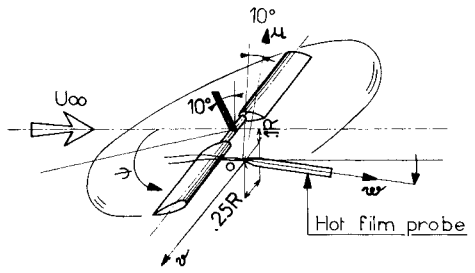

Fig. 1 Orientation system of the probe.

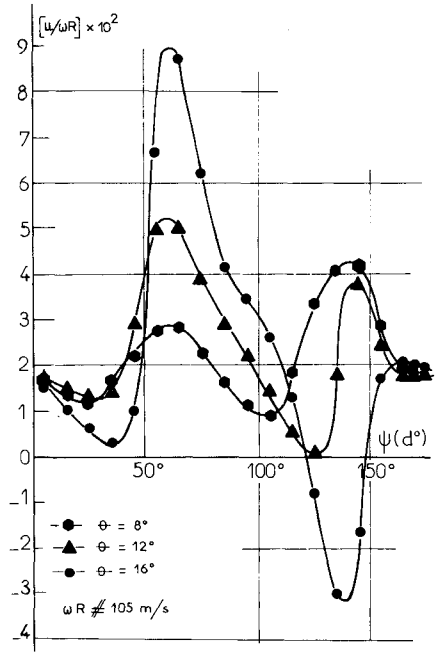

Fig. 2 Azimuthal evolution of $u/\omega R$ with blade pitch.

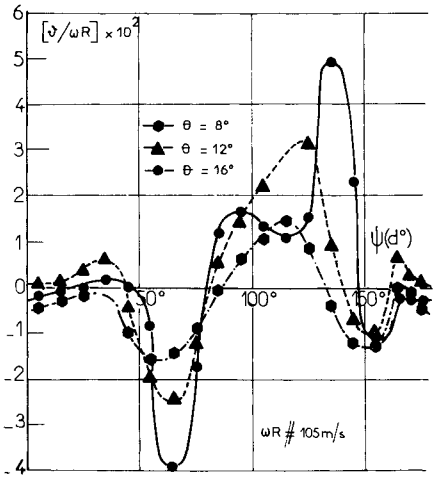

Fig. 3 Azimuthal evolution of $v/\omega R$ with blade pitch.

a flow visualization (obtained by the emission of ammonium chlorate upstream of the rotor) has indicated that this angle condition is fulfilled if the probe is tilted by 10° as shown in Fig. 1. Hence, the method of Ref. 2 enables us to compute the instantaneous velocity components w, u, v (w is along the probe axis, u is in the vertical plane normal to Ow; and v is in the horizontal plane normal to Ow, as shown in Fig. 1). The variations of these components have been plotted vs the azimuthal

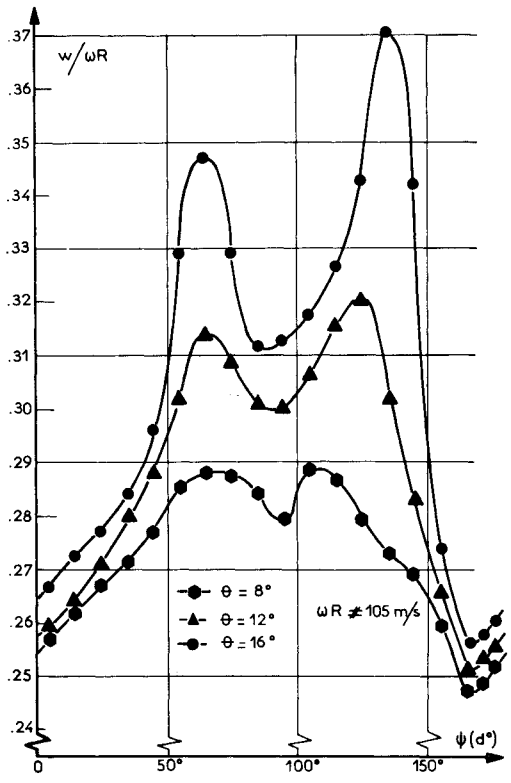

Fig. 4 Azimuthal evolution of $w/\omega R$ with blade pitch.

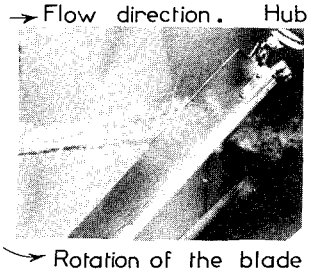

Fig. 5 Top view of the flow around the retreating blade, $\theta = 16°$.

angle ψ which is defined in Fig. 1. The origin of this angle corresponds to the extreme forward position of the blade. For the three values of blade pitch ($\theta = 8°$, 12°, 16°) the results of the measurements of u, v, and w are shown in Figs. 2–4, respectively.

The evolution of the form of $u/\omega R$ with increasing θ, shows (Fig. 2) that the first maximum occurs at a constant value of $\psi \simeq 65°$ for the three value of θ. Each of these maxima is followed by a minimum which decreases in value and increases in azimuth as θ increases. It is interesting to note that the extrema are very strong for $\theta = 16°$.

The variations of $v/\omega R$ (Fig. 3) seem to be inverted in comparison to those of $u/\omega R$. Indeed, the maxima follow the minima at the same values of ψ. However, an unexpected decrease in the value of $v/\omega R$ for $\theta = 16°$ and $\psi \simeq 115°$, can be interpreted as a local stalling of the blade. For the same value of θ, the flow visualization around the blade has been carried out by use of the technique described in Ref. 3. A single emission line splits over the blade. As can be seen on Plate 5, the part of the emission line flowing over the lower side of the blade is slightly deflected towards the tip whereas the part flowing over the upper side is markedly deflected towards the hub. This latter effect is

not observed for smaller values of θ and could perhaps be interpreted as being a consequence of local stall. It should finally be noted that the deflection towards the hub agrees with the sudden drop of $v/\omega R$ observed at $\theta = 16°$.

For the variations of $w/\omega R$ it can be seen in Fig. 4 that a first maximum value is reached at $\psi \simeq 65°$ for all the values of θ. This maximum occurs when the lower side boundary of the blade wake arrives at the probe. This boundary seems to be independent of the pitch blade. The minima observed at $\psi \simeq 90°$ are due to the blade wake and the subsequent maxima correspond to the upper side boundary of the blade wake. These maxima which occur at larger values of ψ for larger θ are significant evidence of the thickening of the wake produced by the separation of the flow on the blade.

It can be concluded that it is possible to infer some phenomena occurring on the blades by analysing the instantaneous velocity measured in the near wake of a helicopter rotor. In particular, the sudden change in the profile of $v/\omega R$ as θ increases very likely indicates some local blade stall and this question will be the object of further investigation.

References

[1] Rebont, J., Maresca, C., and Favier, D., "Mise en Évidence d'un Décollement Local de l'Écoulement sur les Pales d'une Hélice Aérienne," (to be published: comptes rendus de l'Académie des Sciences, Paris).

[2] Favier, D., "Contribution à l'Etude de l'Ecoulement de l'Air à l'Aval d'une Hélice à Partir de Mesures de Vitesse au Film Chaud," Thèse de Spécialité, 1973, Université de Provence, Marseille, France.

[3] Valensi, J., "Etude de l'Écoulement de l'Air Autour d'une Hélice," No. 73, 1935, Publication Scientifique et Technique du Ministère de l'Air, Paris, France.

Technical Comments

Comment on "A Graphical Method for the Investigation of Shock Interference Phenomena"

KARL M. FÖRSTER*
Institute for Aerodynamics, University of Stuttgart, Stuttgart, F.R. Germany

KEEPING abreast of scientific developments in countries other than one's own is becoming more and more difficult. An example of this problem is given by a recent publication in this journal.[1] The graphical method for the straightforward computation of supersonic flow with imbedded, and eventually interacting, shock waves and contact discontinuities described there by Crawford was developed by Weise[2,5] in 1943–1944 as the "Herzkurven-Methode" (the curves resembling the symbolic heart-shape). As encyclopaedic articles[3,4] confirm, Weise tackled not only the same problems as Crawford, but also some others. He also solved the problem of forked, or λ-, shocks.[5-7] Later the Herzkurven-method was used to calculate and classify the types of supersonic flow through cascades,[8] and its basic idea has been adopted for the graphical computation of unsteady one-dimensional flow.[9,3]

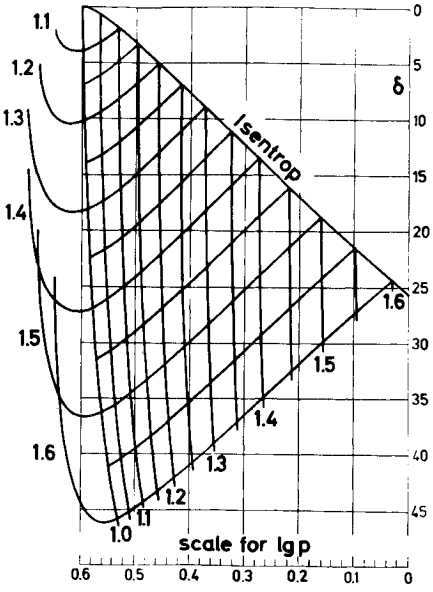

Fig. 1 Herzkurven-diagram after A. Weise, including the isentrop. Laval number ω as parameter, the figures on the left margin giving the characterizing values for the different heart-curves drawn. $\gamma = 1.405$.

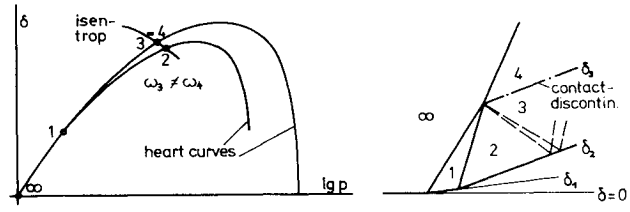

Fig. 2 Flow over double wedge in case of a reflected rarefaction wave.

As to the presentation of the heart-curves, it is neither necessary to plot both (symmetric) halves of the curves nor to ratio the pressure p to a special reference value. The latter is due to the additive feature of the logarithm: $\log(p/p_2) = \log(p/p_1) + \log(p_1/p_2)$, and changing the reference pressure results in nothing but a translation of the figure along the pressure axis without changing the shape. Furthermore, it is advantageous to give a scale of the flow velocity along the heart-curve, preferably in form of the Laval number ω (velocity divided by critical speed, which is the better alternative to the Mach number because of the constancy of the critical speed in isenergic flow). Each heart-curve is then characterized by the Laval number at its cusp which equals the Laval number ahead of the shock. As a last item, we found it convenient to add the isentrop to the log p, δ-diagram (δ angle of streamline), likewise with an ω-scale, and to line up the heart-curves along it in such a way that the location of any cusp on the isentrop's ω-scale corresponds with the characterizing value of that heart-curve. So one set of curves $\omega = \text{const}$ provides the ω-scales for the isentrop and the heart-curves, see Fig. 1. With the help of this universal diagram, the log p, δ-plane for a special flow configuration can

Received January 25, 1974; revision received March 4, 1974.
Index category: Supersonic and Hypersonic Flow.
* Lecturer, Numerical Fluid Mechanics Section.